Indian Journal of Biochemistry & Biophysics
Vol. 62, March 2025, pp. 331-341
DOI: 10.56042/ijbb.v62i3.14131

Camptothecin exerts anti-cancer effects through FoxM1 Inhibition

Pradeep Singh Cheema, Deeptashree Nandi & Alo Nag*

Department of Biochemistry, University of Delhi South Campus, Benito Juarez Marg, New Delhi-110 021, Delhi, India

Received 03 October 2024; *revised 18 December 2024*

Camptothecin (CPT) is primarily known for its anti-cancer effects through the inhibition of topoisomerase I. However, emerging studies suggest that CPT may exert broader effects by targeting other oncogenic pathways. In this study, we explore a novel mechanism by which CPT interacts with FoxM1, a critical transcription factor involved in cancer progression. Our *in silico* docking studies and fluorescence quenching assays demonstrated that CPT and its analogs stably bind to the DNA-binding domain (DBD) of FoxM1. This interaction was further supported by chromatin immunoprecipitation (ChIP) assays, which demonstrated a significant reduction in FoxM1 promoter occupancy and subsequent downregulation of its target genes upon CPT treatment. Electrophoretic mobility shift assays (EMSA) further confirmed that CPT disrupts the binding of purified FoxM1-DBD to its cognate DNA. Importantly, the combination of CPT with Thiostrepton, a known FoxM1 inhibitor, resulted in a marked enhancement of therapeutic efficacy, as evidenced by reduced clonogenic potential and increased apoptosis in cancer cells. The synergistic effect of this combination highlights the potential of CPT to amplify the effectiveness of FoxM1-targeted therapies. Our study elucidates a novel mechanism of action for CPT, expanding its therapeutic potential beyond topoisomerase I inhibition. The findings suggest that FoxM1 levels could be a critical determinant in optimizing CPT-based therapies, and combining CPT with FoxM1 inhibitors may provide a more effective treatment strategy for cancers characterized by FoxM1 overexpression.

Keywords: DNA binding domain, FoxM1 inhibitors, Transcription factor

Since its discovery in 1966 by Wall and Wani[1], Camptothecin (CPT) has been a molecule of significant interest as a potent anti-cancer agent[2]. CPT is a naturally occurring quinoline alkaloid that exerts its anti-cancer effects primarily through the inhibition of DNA topoisomerase I, an enzyme crucial for DNA replication and transcription[3]. Among the derivatives of CPT, Topotecan, Irinotecan and Belotecan are the only FDA-approved CPT analogs currently used in clinical practice for cancer treatment[4-7]. These CPT derivatives have also shown promising outcomes when used in combination with other therapeutic agents for the treatment of various other malignancies[8,9]. Remarkably, there have been reports of complete remission in cases of recurrent cervical cancer with distant metastases following treatment with CPT analogs, underscoring their therapeutic potential[10]. However, despite the clinical success of CPT and its derivatives, several challenges still remain. One of the most significant issues is the considerable treatment-associated toxicities that patients often experience, which can limit the therapeutic use of these compounds[11,12]. Additionally, the emergence of resistance to topoisomerase poisons in cancer cells has become a critical concern, posing another challenge for clinicians. The development of resistance is complex and multifactorial, with one of the major mechanisms being the efflux of drugs by ATP-binding cassette (ABC) transporters[13,14]. These transporters actively pump the drugs out of cancer cells, reducing their intracellular concentration and thereby diminishing their efficacy. Despite extensive research, the exact mechanisms underlying CPT resistance are not fully elucidated, highlighting the need for further investigation.

In light of these challenges, researchers have explored various strategies to overcome CPT resistance and enhance its anti-cancer efficacy. One promising approach is the identification of additional molecular targets of CPT. Several studies have revealed that CPT can modulate the expression and activity of a range of cellular factors, including Polo-like kinase 1 (Plk1), Cyclin B1, vascular endothelial growth factor (VEGF), and hypoxia-inducible factor 1-alpha (HIF-1α)[15-18]. Mechanistically, SN38, an active metabolite of CPT11, has been shown to modulate the levels of Plk1, Cyclin

*Correspondence:
Phone: +91-11-24114159
E-mail: anag@south.du.ac.in

B1 and Chk1 and also downregulate some major mediators of tumor initiation and progression[19-22]. These factors play critical roles in cancer cell proliferation, survival, and angiogenesis, and are often upregulated in various cancers. Interestingly, these cellular factors are established downstream transcriptional targets of the extensively studied oncogenic transcription factor FoxM1[23-26] and thus these reports intrigued us to explore the impact of CPT on FoxM1 mediated carcinogenesis.

FoxM1 has emerged as a master regulator of various cellular processes including cell cycle progression, DNA damage repair, pluripotency, etc., thereby maintaining normal host physiology[27,28]. Moreover, dysregulation of FoxM1 drives cancer initiation, proliferation and sustenance through modulation of angiogenesis, evasion of apoptosis, self-renewal, epithelial-mesenchymal transition, etc[29-33], and thus its aberrant overexpression is closely associated with tumorigenesis, poor prognosis, and resistance to therapy[31,34,35]. Elevated levels of FoxM1 have been implicated in both the initiation and progression of various cancers such as carcinoma of liver, lung, brain, breast, pancreas, colon, ovary, etc.[30,36,37], making it an attractive target for cancer therapy. Studies have consistently demonstrated that the knockdown of FoxM1 in various cancer models leads to a significant reduction in cell proliferation, migration, invasion, and metastasis[38,39]. Additionally, recent findings have shown that downregulation of FoxM1 can re-sensitize drug-resistant cancer cells to chemotherapy[34,40,41], further emphasizing its potential as a therapeutic target. Thus various inhibitors targeting FoxM1 such as Thiostrepton, FDI-6, RCM-1, STL427944, STL001, anti-FoxM1 PROTACs, etc., have been discovered[42-47].

Given the established role of FoxM1 in cancer and the reports suggesting that CPT and FoxM1 share common cellular targets, we were intrigued to investigate whether CPT could influence FoxM1-mediated carcinogenesis. Our research focused on understanding the effect of CPT on FoxM1 expression and activity in cancer cells. Through a series of experiments, we demonstrated that CPT interacts with FoxM1 and reduces the expression levels of FoxM1 and also impairs its transcriptional activity by interfering with its DNA binding capability. This interference likely disrupts the ability of FoxM1 to regulate the transcription of its target genes, thereby hindering the proliferation and survival of cancer cells. Our study provides valuable insights into the mode of action of CPT, expanding its known repertoire of cellular targets to include the critical transcription factor FoxM1. By inhibiting FoxM1, CPT may exert broader anti-cancer effects than previously recognized, offering new avenues for therapeutic intervention.

Materials and Methods

Cell culture, western blotting and antibodies

MCF-7 cells were grown in DMEM medium (Invitrogen, Carlsbad, CA), each supplemented with 10% fetal bovine serum (Invitrogen, Carlsbad, CA), 100 U/mL of penicillin and 100 mg/mL streptomycin (Invitrogen, Carlsbad, CA) in a humidified incubator with 5% CO_2 atmosphere at 37°C. Following treatment with CPT and Thiostrepton, cells were lysed in buffer containing 50 mM Tris-HCl, 400 mM NaCl, 0.2% Nonidet P-40, 10% glycerol and protease inhibitor cocktail (Roche Applied Science, Mannheim, Germany). Equal amounts of whole cell lysates were resolved with SDS-PAGE and subjected to immunoblotting with antibodies against GAPDH, FoxM1, Plk1, Cyclin B1, cleaved PARP antibodies (Santa Cruz, CA), Skp2, Aurora B kinase (Invitrogen, Carlsbad, CA) and cleaved Caspase-7 (Cell Signaling Technology, Denvers, MA).

Real-time polymerase chain reaction

For RNA isolation, MCF-7 cells were treated with 2 μM CPT for 16 h. Total RNA was isolated by using TRIzol reagent (Life Technologies, US) according to the manufacturer's instructions. First strand cDNA was synthesized by using verso cDNA synthesis kit (Thermo Fisher Scientific, US) as per the manufacturer's protocol. PCR was performed using the following sets of primers:

FoxM1b: Sense primer: 5′- GGAGGAAATGCCA CACTTAGCG -3′

Anti-sense primer: 5′- TAGGACTTCTTGGGTCT TGGGGTG -3′

Plk1: Sense primer: 5′- ATCACCTGCCTGACCA TTCCAC -3′

Anti-sense primer: 5′- TCTCCAAGCCTTTATTG AGGACTG -3′

Cyclin B1: Sense primer: 5′- CGGGAAGTCACTG GAAACAT -3′

Anti-sense primer: 5′- AAACATGGCAGTGACA CCAA -3′

GAPDH: Sense primer: 5′- ACCTGACCTGCCGT CTAGAA -3′

Anti-sense primer: 5′- TCCAACCACCCTGTTGC TGTA -3′

Electrophoretic shift mobility assay (EMSA)

EMSA is employed to study the interaction of a transcription factor (protein) with its target DNA binding motif[48]. In order to determine the specificity of CPT for inhibiting the interaction of FoxM1-DBD to its consensus sequencea Cy5 labeled oligo (5-Cy5-AAACAAACAAACAAACAAACAAACAATC-3) was commercially synthesized (IDT, Coralville, IA). Purified His-tagged DNA binding domain of FoxM1 (His-DBD) was allowed to bind to the Cy5 labeled consensus promoter sequence in a 20 µL reaction mixture containing 20 mM Tris-Cl (pH 7.5), 100 mM KCl, 1 mM $MgCl_2$, 10% glycerol, and 0.01 mg/mL BSA. For the competition reactions the indicated doses of CPT were incubated with His-DBD for 30 min at RT followed by incubation with labeled oligo for 45 min. The reaction mix was then loaded onto a 5% TBE native gel and resolved at 125 volts at 4°C followed by imaging on a FLA-9000 image analyzer.

Chromatin immunoprecipitation assay (ChIP assay)

ChIP assay is a crucial technique which is utilized to study the binding of a transcription factor to its target DNA within the cells[49]. In our study, MCF-7 cells were grown in 100 mm^2 dishes to 70% confluence prior to treatment with either DMSO or 2 µM CPT for 6 h. The treated cells were cross-linked with 1% formaldehyde at room temperature for 20 min and quenched with 125 mM glycine. Cells were harvested by scraping into cold PBS and then lysed in ChIP lysis buffer (50 mM Tris pH 8.1, 1% SDS, 1 mM EDTA) supplemented with protease inhibitor cocktail (Roche). The samples were sonicated using a microtip sonicator (Misonix) for 10 min at amplitude of 40 with a pulse of 2 sec ON/10 sec OFF. The sonicated samples were then centrifuged at 20,000 g for 15 min at 4°C. The clear supernatant was divided equally and incubated overnight with 1 µg of anti-FoxM1 antibody or anti-rabbit IgG which was used as a negative control. Following incubation the antibody-protein complex was pulled down with protein A beads for 3 h and the beads were washed sequentially with low salt buffer (50 mM Tris pH 8.0, 150 mM NaCl, 0.01% SDS, 1% Triton X-100 and 1 mM EDTA) and high salt buffer (50 mM Tris pH 8.0, 500 mM NaCl 0.01% SDS, 1% TritonX-100 and 1 mM EDTA,). Bound DNA was eluted by rocking with elution buffer (50 mM NaCl, 1% SDS, 8 mg/mL $NaHCO_3$) at RT for 30 min. The eluent was reverse crosslinked by incubation at 65°C overnight followed by ethanol precipitation of the samples. The DNA pellet was air dried and resuspended in 200 µL sterile water containing 5 µg/µL proteinase K and incubated at 37°C for 30 min. The samples were then precipitated by phenol chloroform method and the pellet was air dried and resuspended in 30 µL DNase free water. PCR was carried out using 4 µL of purified DNA in a 10 µL reaction volume using the following primers:

Cyclin B1: Sense primer: 5′- CGGGAAGTCACTG GAAACAT

Anti-sense primer: 5′- AAACATGGCAGTGACA CCAA -3′

Cdc25B: Sense primer: 5′- AAGAGCCCATCAGT TCCGCTTG -3′

Anti-sense primer: 5′- CCCATTTTACAGACCTG GACGC -3′

Aurora B kinase: Sense primer: 5′- GCAACGAAA GGTCTTGGTGG -3′

Anti-sense primer: 5′- TCTAACTTCTCTGCCCG ATGGAG -3′

GAPDH: Sense primer: 5′- ACCTGACCTGCCGT CTAGAA -3′

Anti-sense primer: 5′- TCCAACCACCCTGTTGC TGTA -3′

The PCR cycle conditions were: 95°C for 10 min followed by 30 cycles of 30 sec at 95°C, 30 sec at 60°C and 30 sec at 72°C.

FoxM1-His-DBD purification

E. coli BL21 (λDE3) competent cells and the transformed cells were grown at 37°C, 180 rpm until an O.D (596 nm) of 0.8 was obtained. The culture was then induced with 0.5 mM IPTG for 5 h at 25°C. The induced culture was then centrifuged at 5000 rpm for 15 min and the obtained pellet was then resuspended into lysis buffer (50 mM Tris (pH 8.0), 300 mM NaCl, 1 mM PMSF, 0.1 mg/mL lysozyme). The lysate was sonicated (Amp 40; ON time: 5 sec; OFF time: 15 sec) for 4 min and then centrifuged to obtain a clear supernatant which was then allowed to bind to Ni-NTA resin under the flow of gravity. The beads were washed, and the bound protein was eluted with lysis buffer containing 500 mM imidazole. The obtained fraction was subjected to gel filtration chromatography to obtain pure His-DBD fractions.

Fluorescence spectroscopy

Quenching of the fluorescence of macromolecules such as proteins can occur upon binding of ligands such as small molecules and this change in the fluorescence can be studied by utilizing fluorescence spectroscopy[50]. In order to investigate the impact of binding of CPT to the fluorescence of His-DBD, fluorescence measurements were done on a Cary Eclipse Varian spectrophotometer (Varian Inc., Santa Clara, CA, USA) at a constant temperature of 25°C. The concentration of His-DBD was 10 µM for fluorescence experiments and the range of concentration for CPT was 1–100 µM. For tryptophan specific fluorescence, His-DBD was excited at 292 nm and emission was recorded in the range of 300-500 nm with a 5 nm slit width for excitation and emission. K_D values of the compounds were determined by plotting the double reciprocal plot of ΔF (difference in fluorescence) versus [I] (CPT concentration). DMSO (0.4%) was used for background reference and all the experiments were performed in triplicates.

Cell viability assay

Cells were seeded in triplicates in 96 well plates and allowed to grow for 24 h followed by incubation with Thiostrepton alone or in combination with CPT at varying concentrations. After 24 h of treatment, 20 µL of MTT solution (5 mg/mL in PBS, Sigma, St. Louis, MO) was added to each well and incubated for 4 h. MTT solution was subsequently removed from wells and resulting formazan crystals were solubilized in 100 µL DMSO by rocking gently for 15-30 min at RT. Optical density of the dissolved formazan was measured using a Tecan microplate reader (Infinite M200 Pro) at 570 nm. Experiments were performed in triplicates and results were calculated as averages ± SD of at least three independent experiments.

Clonogenic assay

A total of 1000 cells per well were seeded in a 12-well plate and allowed to grow in complete medium for 24 h. The cells were then incubated with growth medium containing the indicated dose of Thiostrepton and CPT for the next 24 h in a CO_2 incubator at 37°C. Following incubation, the media was replaced with normal media and the cells were allowed to grow for 10 days until they formed colonies with substantially good size (>50 cells per colony). Once the colonies were formed, they were fixed in 100% methanol and stained with 0.5% crystal violet in 25% methanol. Excess stain was washed off using tap water. The retained dye was eluted in dye extraction buffer (0.5% SDS, 50% ethanol and 0.5 M Tris-Cl pH 7.8). The intensity of the eluted dye was determined by absorbance measurement at 588 nm.

***In silico* analysis**

The crystal structure of FoxM1-DBD was downloaded from RCSB protein data bank (PDB ID: 3G73)[51] and the structure of the ligands were obtained from pubchem. Docking was performed by utilizing the swissdock software from expasy[52]. The docked pdb files were utilized for generation of the representative stick and ribbon model of CPT and its analogs using PyMOL software (Schrödinger, LLC, New York). The residue interaction map was generated by employing Maestro 10.4 software (Maestro, Schrödinger, LLC, New York).

Statistical analysis

The experiments were repeated three times unless otherwise mentioned. For statistical significance Student's *t*-test was utilized for comparison of the data sets and represented as mean ± S.D. Statistical significance was indicated with *P*- values * ≤ 0.05, **≤0.01, *** ≤0.001.

Results

***In silico* validation of the association of CPT with FoxM1-DBD**

To investigate the interaction of CPT with FoxM1 DBD and its potential to interfere with the DNA binding ability of FoxM1, we conducted a docking study involving CPT and its clinically relevant analogs, Topotecan and Irinotecan. We docked the compounds onto the available crystal structure of the FoxM1-DBD to perform a comparative analysis of their interactions. The results revealed that CPT and its analogs not only established stable interactions with the DBD but also formed hydrogen bonds with key residues (Table 1). These findings suggest that the binding of these compounds could potentially disrupt and FoxM1-DNA interaction and thus obstruct its transactivation functions (Fig. 1).

Further, we performed an in-depth analysis of the interacting residues by generating a detailed residue interaction map using Maestro software. This analysis provided a clearer understanding of the specific molecular interactions involved. Notably, we observed that CPT and its analogs docked near the basic amino acids within the DBD, which are critical for the DNA binding function of FoxM1. The

Table 1 — Summary of various *in silico* binding parameters of CPT and its analogs

S. No.	Binding parameters	CPT	Topotecan	Irinotecan
1.	Binding energy (ΔG) (Cal/mol)	-6.85	-7.53	-7.26
2.	No. of hydrogen bonds	1	1	1
3.	No. of basic amino acid residues in vicinity	3	2	4

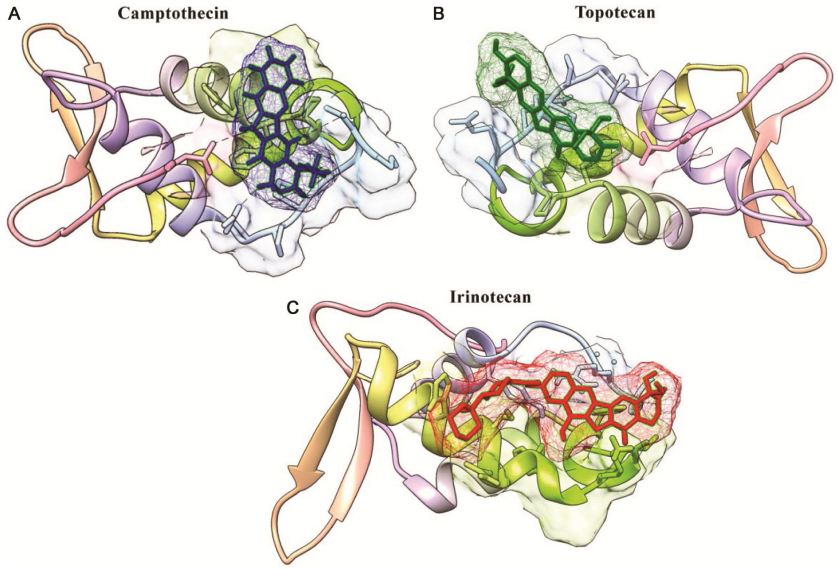

Fig. 1 — *In silico* analysis of the interaction of CPT and its analogs against DNA Binding Domain (DBD) of FoxM1. (A-C) The images represent 3D stick model of (A) CPT; (B) Topotecan; and (C) Irinotecan docked to the crystal structure of FoxM1-DBD (represented by the ribbon model)

proximity to these positively charged residues implies that the binding of CPT and its analogs could reasonably interfere with the electrostatic interactions that FoxM1 relies on for stable DNA binding (Fig. 2). This potential disruption could underlie the mechanism by which CPT and its analogs exert their anti-cancer effects through the inhibition of FoxM1's transcriptional activity.

CPT associates physically with the DNA binding domain of FoxM1

Further, to verify the direct interaction of the CPT with His-DBD, we performed tryptophan specific fluorescence quenching analysis by utilizing fluorescence spectroscopy. This technique was chosen because it allows for the detection of changes in the environment surrounding tryptophan residues, which are sensitive to conformational alterations upon ligand binding. To achieve this, 10 µM of His-DBD was incubated with various doses of CPT and fluorescence intensity of the tryptophan residues was measured. As observed in (Fig. 3A & B), a noticeable quenching of the tryptophan specific fluorescence was visible, which indicated that the physical interaction of CPT with His-DBD induces conformational changes in the protein, likely affecting its structural stability. Moreover, we observed a substantial dose dependent reduction in the fluorescence intensity which revealed a dissociation equilibrium constant (K_D) of 7.7 µM (Fig. 3C) thereby indicating a strong binding affinity between CPT and His-DBD. Overall, these findings suggest that CPT physically interacts with and de-stabilizes the protein structure of FoxM1-His-DBD.

Assessing the impact of Camptothecin on the levels FoxM1 and its downstream targets

After confirming the interaction between CPT and FoxM1-DBD and considering existing literature that suggests CPT and FoxM1 share common cellular targets, we were intrigued to explore the potential impact of CPT on cellular FoxM1 levels. To investigate this, we treated the MCF-7 breast cancer cells with increasing concentrations of CPT for 16 h. Following treatment, FoxM1 protein levels and the expression of its downstream target genes were analyzed *via* immunoblotting. This approach aimed to determine whether CPT modulates FoxM1 expression and its associated signaling pathways, thereby providing insights into the molecular mechanisms underlying CPT's anti-cancer activity.

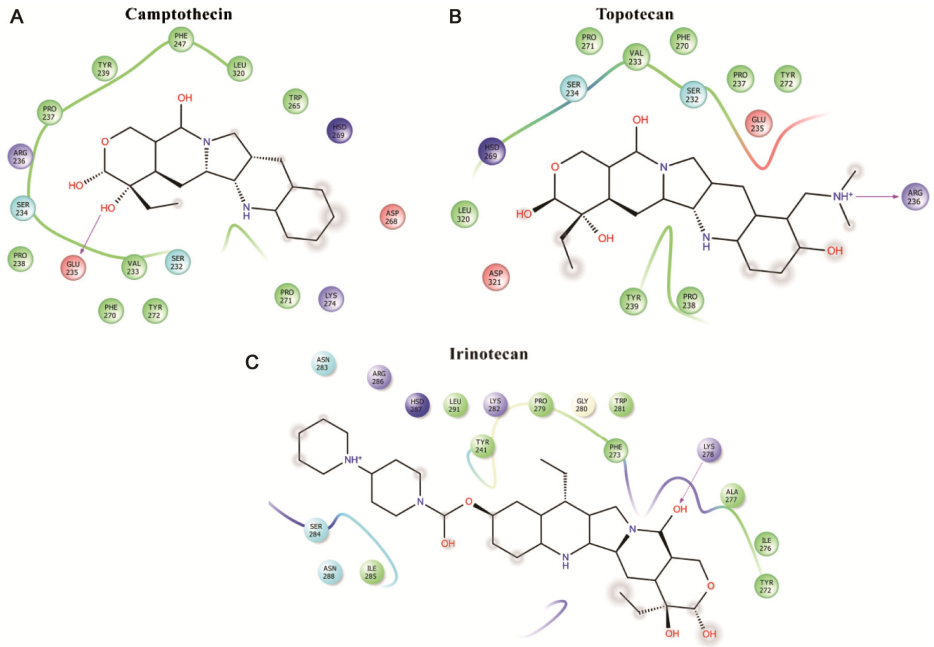

Fig. 2 — Interaction maps of CPT and its analogs docked to FoxM1-DBD. (A) CPT; (B) Topotecan; and (C) Irinotecan. Maestro 10.4 software was used to assess the interacting residues of the docked ligands. These compounds were also found to interact with FoxM1-DBD by forming a hydrogen bond, although with different amino acid residues (Table 1)

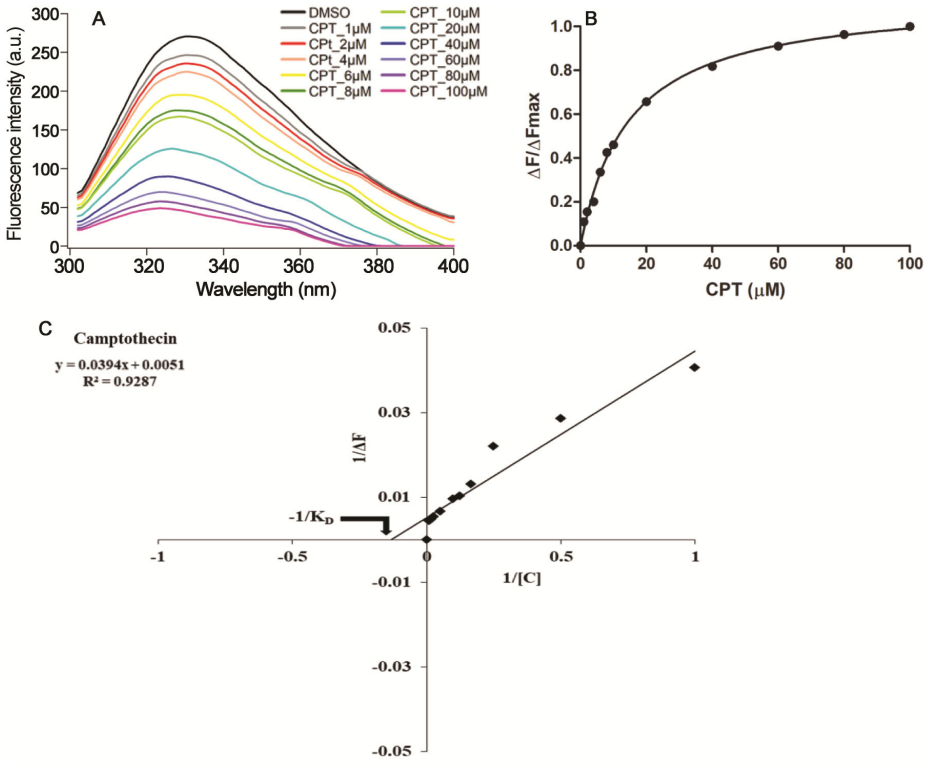

Fig. 3 — Assessing the binding of CPT to purified His-DBD. Interaction of CPT with His-DBD alters its intrinsic tryptophan fluorescence. (A) Purified His-DBD (10 μM) was titrated with the indicated doses of CPT and the fluorescence intensity was recorded (λ_{max} at 292 nm, λ_{em} 300 - 400 nm); (B) The fraction change in the fluorescence intensity ($\Delta F/\Delta F_{max}$) with increasing concentration (represented as a black dot for each concentration of 0,1,2,4,6,8,10,20,40,60,80 and 100 μM) of the CPT was presented graphically; (C) Double reciprocal plot for CPT. The intercept of the straight line on x-axis provides $-1/K_D$ values from which K_D values were calculated

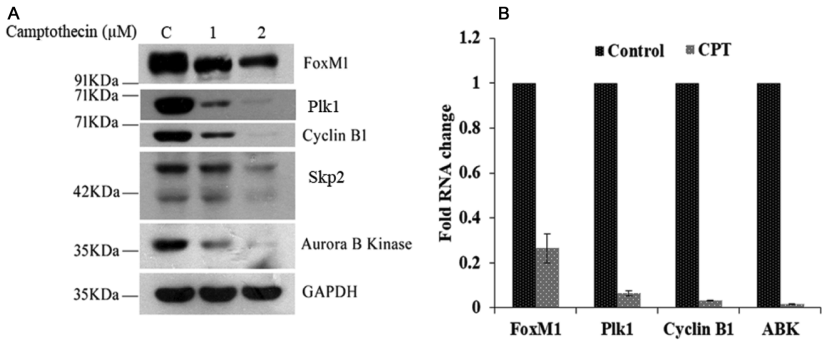

Fig. 4 — Camptothecin diminishes FoxM1 levels. (A) MCF-7 cells were treated for 16 h with the indicated doses of CPT. Following incubation, the treated cells were harvested and lysed. The lysate was then resolved on SDS-PAGE followed by immunoblotting with antibodies against FoxM1, Plk1, CyclinB1, Skp2, Aurora B kinase and GAPDH. GAPDH was used as a loading control; and (B) MCF-7 cells were incubated with 2 μM dose of CPT for 8 h followed by TRizol lysis to obtain mRNA. cDNA was prepared from the mRNA and subjected to Real time PCR analysis. Fold mRNA change was calculated from the obtained Ct values and represented graphically

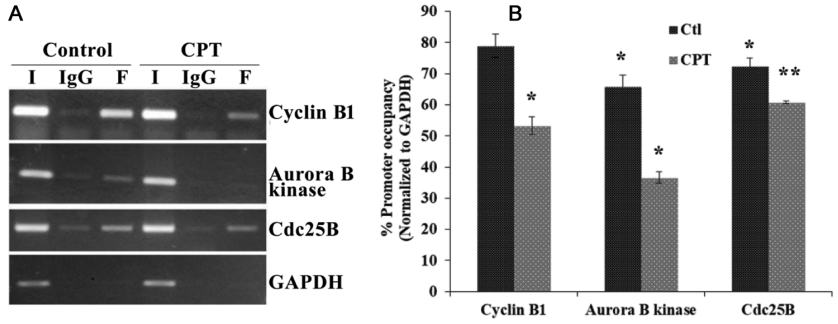

Fig. 5 — CPT effectively hampers FoxM1 promoter occupancy. (A) Equal numbers of MCF-7 cells were treated with CPT for 6 h and processed for chromatin immunoprecipitation. The obtained chromatin was then subjected to ChIP-PCR with target primers and resolved on a 0.8% TAE gel; and (B) The obtained PCR products were quantified using Image J software and represented graphically. Students *t* test was utilized to compare the data sets (p-value * ≤ 0.05)

Interestingly, we observed a significant reduction in the levels of FoxM1 in a dose dependent manner which was also reflected on the protein levels of its sub-ordinate genes Plk1, Cyclin B1, Skp2 and Aurora B kinase (Fig. 4A). This verified that CPT targets FoxM1 in the cells and points to the possibility that apart from the conventional known mode of action of targeting Toposisomerase I, it may have previously unexplored functions as well. To further support this notion, we also studied the impact of CPT on the transcript levels of FoxM1 and its target genes. Treatment with CPT resulted in a marked decrease in the mRNA levels of FoxM1 and its target genes Plk1, Cyclin B1 and Aurora B kinase (Fig. 4B). Thus, CPT significantly represses FoxM1 at its transcript level, which leads to downregulation of its target genes as well. It is, therefore, safe to propose that CPT may lead to cell cycle inhibition by targeting these factors apart from topoisomerase I in the cancer cells.

Determining the effect of CPT on promoter occupancy of FoxM1

To investigate whether CPT affects the promoter-binding ability of FoxM1, in addition to its transcriptional downregulation, we conducted a chromatin immunoprecipitation (ChIP) assay on MCF-7 cells treated with CPT. Since FoxM1 is a key transcriptional regulator of several cell cycle-related genes, any disruption in its promoter occupancy should directly impact the expression levels of its target genes. Our ChIP assay results revealed a significant reduction in the promoter occupancy of FoxM1, as evidenced by the decreased levels of Cyclin B1, Aurora B kinase, and Cdc25B (Fig. 5A & B). These findings further strengthened our hypothesis that CPT hampers the transactivation function of FoxM1.

Evaluating the ability of CPT to obstruct the binding of FoxM1-DBD to its consensus DNA motif

Building on our observation that CPT reduces the promoter occupancy of FoxM1 in cells, we further

validated this effect *in vitro* using an electrophoretic mobility shift assay (EMSA). For this experiment, His-tagged FoxM1-DBD protein was purified from a heterologously expressed pET28a (+) DBD construct. The purified DBD was then incubated with varying concentrations of CPT, followed by the addition of a Cy5-labeled oligonucleotide to form DNA-protein complexes. These complexes were analysed using native electrophoresis.

We observed a dose-dependent decrease in complex formation in the presence of CPT, with a reduction in the intensity of the bound oligonucleotide by 17% at a 0.2 µM dose and 23.5% at a 2 µM dose (Fig. 6A & B). Although modest, this significant decline (p value = 0.029164 for 2 µM dose) in the ability of DBD to bind its cognate DNA reinforces the previously observed reduction in FoxM1's promoter occupancy. Collectively, these results suggest that CPT exerts its anti-cancer effects, at least in part, by impairing the DNA recognition capability of FoxM1.

Evaluating the impact of combination of CPT with Thiostrepton on its anti-cancer properties

Next, we sought to determine the physiological effect of this novel mode of action of CPT by conducting a colony formation assay with CPT alone and in combination with Thiostrepton, a known FoxM1 inhibitor. Both CPT and Thiostrepton individually demonstrated cytotoxic effects, significantly reducing the cells' ability to form colonies. However, when used together, the reduction in colony formation was even more pronounced (Fig. 7A). Specifically, Thiostrepton alone reduced colony formation to 39.11% and 32.59% at the respective doses, while CPT alone decreased it to 36.47%. Remarkably, the combination of Thiostrepton with CPT led to a substantial decrease in the clonogenic potential, reducing it to 8.73% and 3.19%, respectively, (Fig. 7B). These findings suggest that CPT potentiates the anti-cancer effects of Thiostrepton by further inhibiting FoxM1.

Furthermore, we also assessed the impact of this combination on the cell viability of MCF-7 cells by MTT assay. MCF-7 cells were treated with different doses of Thiostrepton alone or in combination with 0.5 µM CPT.

The results revealed a substantially greater decrease in cell viability when Thiostrepton was used in combination with CPT, as opposed to using Thiostrepton by itself. (Fig. 8A). Notably, the IC_{50} value of Thiostrepton decreased approximately 5-fold, from 10.5 µM to 2.4 µM, when combined with CPT. Additionally, the combination treatment further induced apoptosis, as evidenced by increased cleavage

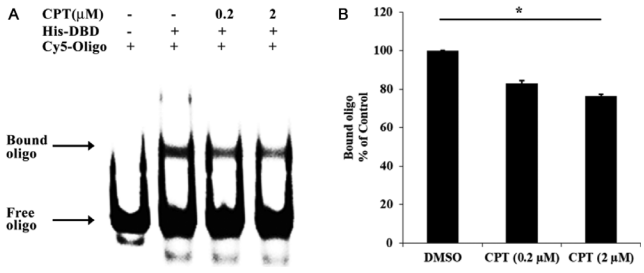

Fig. 6 — CPT obstructs the binding of His-DBD to its cognate DNA. (A) Purified His-DBD was incubated with the indicated doses of CPT for 30 min and then allowed to bind to the Cy5-labeled consensus oligo for next 45 min. Upon incubation the complexes were resolved on a 5% TBE gel; and (B) The intensity of the bound oligo was quantified using ImageJ software and represented graphically. The experiments were repeated twice and error bars indicate S.D. (p-value *<0.05)

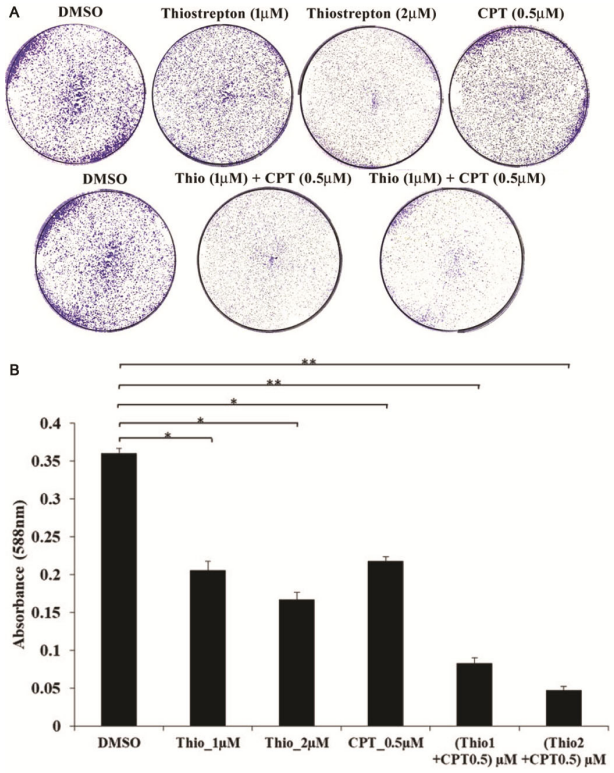

Fig. 7 — CPT sensitizes cancer cells to the effect of Thiostrepton: (A) Equal number of MCF-7 cells were seeded for colony formation assay. The cells were treated with the indicated doses of Thiostrepton and CPT either alone or in combination for 24 h. Following treatment, they were allowed to grow in normal media and form colonies for a week. After a week, the obtained colonies were fixed and stained with 0.5% crystal violet dye; and (B) The crystal violet stain that was retained by the colonies was eluted and absorbance was measured at 588 nm. The relative absorbance was represented graphically

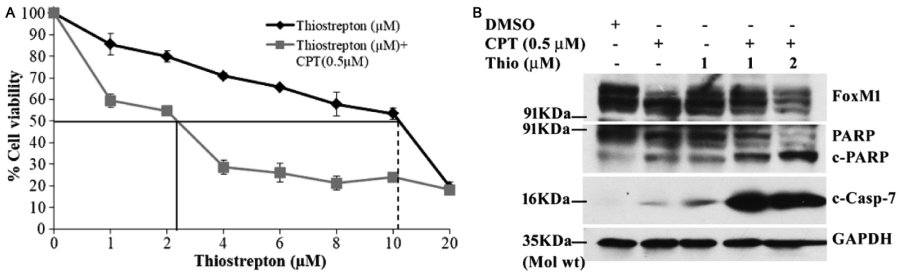

Fig. 8 — CPT enhances the efficacy of Thiostrepton (A) Cell viability assay. For MTT assay, 5000 cells per well seeded in a 96-well plate followed by incubation with Thiostrepton either alone or in combination with 0.5 μM dose of CPT. After 24 h of treatment, the media containing drugs was removed and the cells were incubated with MTT for 4 h. Following incubation, the formazan crystals were dissolved in DMSO, and absorbance was recorded at 570 nm. The cell viability was represented graphically as percentage of control; and (B) Equal number of MCF-7 cells was treated with either DMSO or with indicated doses of CPT or Thiostrepton alone or in combination. Treated cells were lysed and the lysates were then resolved on SDS-PAGE followed by immunoblotting with antibodies against FoxM1, cleaved PARP, cleaved caspase-7 and GAPDH

of apoptotic markers PARP and caspase-7 (Fig. 8B) and a significant reduction in cell viability. This enhanced apoptotic response reinforces the notion that the anti-FoxM1 activity of CPT not only potentiates Thiostrepton's effects but also contributes to a more robust growth-suppressive effect on cancer cells.

Discussion

Camptothecin (CPT) has long been recognized as an effective inhibitor of topoisomerase I, a mechanism that has historically been considered its sole mode of action. However, recent studies have expanded our understanding of CPT's effects, revealing its involvement in downregulating various oncogenic factors such as VEGF, HIF-1α, Plk1, and Cyclin B1, which are involved in different oncogenic processes[15,16,18]. Through this study we have explored a potentially novel mechanism by which CPT exerts its anti-cancer effects, specifically focusing on its interaction with FoxM1, a critical transcription factor implicated in cancer progression. Our computational docking studies and subsequent fluorescence quenching experiments provided compelling evidence that CPT and its analogs bind stably to the DNA-binding domain (DBD) of FoxM1 (Figs 1 & 2). The observed decrease in tryptophan-specific fluorescence upon CPT binding confirmed a physical interaction between CPT and FoxM1-DBD, leading to conformational changes in the protein (Fig. 3). This direct biochemical interaction supports our hypothesis that CPT interferes with FoxM1's transcriptional activity by obstructing its ability to bind DNA and regulate gene expression critical for cancer cell proliferation and survival. This interaction-based mechanism of action could explain the broad anti-cancer efficacy of CPT, particularly in cancers where FoxM1 is overexpressed. Therefore, our fluorescence quenching results significantly strengthen the proposition that CPT disrupts FoxM1 function through direct binding to its DBD, offering valuable insights into its mode of action as a potential therapeutic agent.

Further investigations revealed that CPT treatment of MCF7 cells caused reduction in the levels of FoxM1 at both protein and mRNA levels, suggesting a potential anti-FoxM1 activity of CPT (Fig. 4). This reduction was corroborated by ChIP assays, which showed diminished FoxM1 promoter occupancy and reduced gene expression of downstream targets (Fig. 5). To further validate this observation, EMSA was employed to assess the direct impact of CPT on FoxM1 DNA-binding activity. The EMSA results demonstrated a dose-dependent reduction in the formation of DNA-protein complexes, with a notable decrease in the intensity of bound oligonucleotides (Fig. 6). This decline in DNA-binding ability supports our ChIP assay findings and indicates that CPT interferes with FoxM1's capacity to recognize and bind its target DNA sequences. These results collectively indicate that CPT indeed interacts with FoxM1, which sharply hinders its transactivation function, thereby impeding tumorigenesis-related processes driven by FoxM1.

The physiological implications of these findings were evaluated through colony formation assays and MTT assays. Treatment with CPT alone and in combination with Thiostrepton, a known FoxM1 inhibitor, both resulted in reduced colony formation. However, the combinatorial treatment with CPT and Thiostrepton led to a significantly greater decline in clonogenic potential, highlighting a synergistic effect. However, given the various modes of action of Thiostrepton in inhibiting FoxM1, it would require additional investigation to validate this observation which can form part of a future

study including other derivatives of CPT as well. The combination also resulted in a dramatic reduction in the IC_{50} value of Thiostrepton, underscoring the role of CPT in enhancing the efficacy of FoxM1 inhibition (Fig. 7). This combinatorial approach not only improved the efficacy of Thiostrepton but also increased the induction of apoptosis, as evidenced by a substantial reduction in cell viability and increased cleavage of apoptotic markers PARP and caspase-7 (Fig. 8). This synergistic effect underscores the potential of CPT to enhance the anti-cancer efficacy of existing FoxM1 inhibitors.

Our findings highlight the critical role of FoxM1 in CPT-based chemotherapy, suggesting that assessing FoxM1 levels could be crucial for predicting treatment outcomes and personalizing therapy. The ability to target FoxM1 more effectively could be particularly valuable in overcoming drug resistance and improving patient outcomes. By integrating FoxM1 inhibitors along with CPT-based chemotherapeutics, it may be possible to enhance the overall effectiveness of cancer treatments and potentially increase survival rates. This study presents novel insight into the mechanism of action of CPT, which can aid in improving its efficacy and overall survival of the cancer patients by enhancing the effectiveness of CPT based chemotherapeutics.

Acknowledgement

AN lab is supported by research grants from Faculty Research Program Grant from Institution of Eminence, University of Delhi (Ref. No./IoE/2024-25/12/FRP and Ref. No./IoE/2023-24/12/FRP), CRG Grant from DST SERB (CRG/2020/003380), DBT Grant (BT/PR15422/MED/30/1705/2016), CSIR EMR Grant 27/0388/23/EMR-II. Financial support from CSIR and DBT for providing fellowships to PSC and DN, respectively, is thankfully acknowledged.

Conflict of interest

All authors declare no conflicts of interest.

References

1 Wall ME, Wani MC, Cook Ca, Palmer KH, McPhail Aa & Sim G, Plant antitumor agents. I. The isolation and structure of camptothecin, a novel alkaloidal leukemia and tumor inhibitor from camptotheca acuminata1, 2. *J Am Chem Soc*, 88 (1966) 3888.

2 Hsiang YH & Liu LF, Identification of mammalian DNA topoisomerase I as an intracellular target of the anticancer drug camptothecin. *Cancer Res*, 48 (1988) 1722.

3 Avemann K, Knippers R, Koller T & Sogo JM, Camptothecin, a specific inhibitor of type I DNA topoisomerase, induces DNA breakage at replication forks. *Mol Cell Biol*, 8 (1988) 3026.

4 Liu YQ, Li WQ, Morris-Natschke SL, Qian K, Yang L, Zhu GX, Wu XB, Chen AL, Zhang SY & Nan X, Perspectives on biologically active camptothecin derivatives. *Med Res Rev* 35 (2015) 753.

5 Lee D, Kim SW, Suh C, Lee JS, Lee J, Lee SJ, Ryoo B, Park K, Kim J & Heo D, Belotecan, new camptothecin analogue, is active in patients with small-cell lung cancer: results of a multicenter early phase II study. *Ann Oncol*, 19 (2008) 123.

6 Takimoto CH & Arbuck S, Clinical status and optimal use of topotecan. *Oncology (Williston Park, NY)*, 11 (1997) 1635.

7 Fujita Ki, Kubota Y, Ishida H & Sasaki Y, Irinotecan, a key chemotherapeutic drug for metastatic colorectal cancer. *World J Gastroenterol*, 21 (2015) 12234.

8 Perez EA, Hillman DW, Mailliard JA, Ingle JN, Ryan JM, Fitch TR, Rowland KM, Kardinal CG, Krook JE & Kugler JW, Randomized phase II study of two irinotecan schedules for patients with metastatic breast cancer refractory to an anthracycline, a taxane, or both. *J Clin Oncol*, 22 (2004) 2849.

9 Mirchandani D, Hochster H, Hamilton A, Liebes L, Yee H, Curtin JP, Lee S, Sorich J, Dellenbaugh C & Muggia FM, Phase I study of combined pegylated liposomal doxorubicin with protracted daily topotecan for ovarian cancer. *Clin Can Res*, 11 (2005) 5912.

10 Kaneki T, Koizumi T, Kawashima A, Tsushima K, Kubo K, Fujimoto K, Honda T & Akamatsu T, Double cancer (lung and colon cancer) that showed complete remission with irinotecan and cisplatin combined chemotherapy. *J Gastroenterol*, 35 (2000) 864.

11 Venditto VJ & Simanek EE, Cancer therapies utilizing the camptothecins: a review of the in vivo literature. *Mol Pharm*, 7 (2010) 307.

12 Tomicic MT & Kaina B, Topoisomerase degradation, DSB repair, p53 and IAPs in cancer cell resistance to camptothecin-like topoisomerase I inhibitors. *Biochim Biophys Acta Rev Cancer*, 1835 (2013) 11.

13 Rasheed ZA & Rubin EH, Mechanisms of resistance to topoisomerase I-targeting drugs. *Oncogene*, 22 (2003) 7296.

14 Lepper ER, Nooter K, Verweij J, Acharya MR, Figg WD & Sparreboom A, Mechanisms of resistance to anticancer drugs: the role of the polymorphic ABC transporters ABCB1 and ABCG2. *Pharmacogenomics*, 6 (2005) 115.

15 Kamiyama H, Takano S, Tsuboi K & Matsumura A, Anti-angiogenic effects of SN38 (active metabolite of irinotecan): inhibition of hypoxia-inducible factor 1 alpha (HIF-1α)/ vascular endothelial growth factor (VEGF) expression of glioma and growth of endothelial cells. *J Cancer Res Clin Oncol*, 131 (2005) 205.

16 Janss AJ, Maity A, Tang CB, Muschel RJ, McKenna WG, Sutton L & Phillips PC, Decreased cyclin B1 expression contributes to G2 delay in human brain tumor cells after treatment with camptothecin. *Neuro Oncol*, 3 (2001) 11.

17 Clements MK, Jones CB, Cumming M & Daoud SS, Antiangiogenic potential of camptothecin and topotecan. *Cancer Chemother Pharmacol*, 44 (1999) 411.

18 Zuco V, De Cesare M, Zaffaroni N, Lanzi C & Cassinelli G, PLK1 is a critical determinant of tumor cell sensitivity to CPT11 and its inhibition enhances the drug antitumor efficacy in squamous cell carcinoma models sensitive and resistant to camptothecins. *Oncotarget*, 6 (2015) 8736.

19 Tse AN & Schwartz GK, Potentiation of cytotoxicity of topoisomerase i poison by concurrent and sequential treatment with the checkpoint inhibitor UCN-01 involves

disparate mechanisms resulting in either p53-independent clonogenic suppression or p53-dependent mitotic catastrophe. *Cancer Res*, 64 (2004) 6635.

20 Levesque AA, Kohn EA, Bresnick E & Eastman A, Distinct roles for p53 transactivation and repression in preventing UCN-01-mediated abrogation of DNA damage-induced arrest at S and G2 cell cycle checkpoints. *Oncogene*, 24 (2005) 3786.

21 Kumar S & Sherman MY, Resistance to TOP-1 inhibitors: good old drugs still can surprise us. *Int J Mol Sci*, 24 (2023) 7233.

22 Dai Y, Qian M & Li Y, Structural Modification Endows Small-Molecular SN38 Derivatives with Multifaceted Functions. *Molecules*, 28 (2023) 4931.

23 Dibb M, Han N, Choudhury J, Hayes S, Valentine H, West C, Ang Y & Sharrocks A, The FOXM1-PLK1 axis is commonly upregulated in oesophageal adenocarcinoma. *Br J Cancer*, 107 (2012) 1766.

24 Leung TW, Lin SS, Tsang AC, Tong CS, Ching JC, Leung WY, Gimlich R, Wong GG & Yao KM, Over-expression of FoxM1 stimulates cyclin B1 expression. *FEBS Lett*, 507 (2001) 59.

25 Zhang Y, Zhang N, Dai B, Liu M, Sawaya R, Xie K & Huang S, FoxM1B transcriptionally regulates vascular endothelial growth factor expression and promotes the angiogenesis and growth of glioma cells. *Cancer Res*, 68 (2008) 8733.

26 Zhang R, Tao F, Ruan S, Hu M, Hu Y, Fang Z, Mei L & Gong C, The TGFβ1-FOXM1-HMGA1-TGFβ1 positive feedback loop increases the cisplatin resistance of non-small cell lung cancer by inducing G6PD expression. *Am J Transl Res*, 11 (2019) 6860.

27 Jaiswal N, Chakraborty S & Nag A, Biology of FOXM1 and its emerging role in cancer therapy. *J Proteins Proteomics*, 5 (2014) 1.

28 Liao GB, Li XZ, Zeng S, Liu C, Yang SM, Yang L, Hu CJ & Bai JY, Regulation of the master regulator FOXM1 in cancer. *Cell Commun Signal*, 16 (2018) 57.

29 Khan MA, Khan P, Ahmad A, Fatima M & Nasser MW, FOXM1: A small fox that makes more tracks for cancer progression and metastasis. *Semin Cancer Biol*, 92 (2023) 1.

30 Kong X, Li L, Li Z, Le X, Huang C, Jia Z, Cui J, Huang S, Wang L & Xie K, Dysregulated expression of FOXM1 isoforms drives progression of pancreatic cancer. *Cancer Res*, 73 (2013) 3987.

31 Zona S, Bella L, Burton MJ, de Moraes GN & Lam EWF, FOXM1: an emerging master regulator of DNA damage response and genotoxic agent resistance. *BBA-Gene Regul Mech*, 1839 (2014) 1316.

32 Wen N, Wang Y, Wen L, Zhao SH, Ai ZH, Wang Y, Wu B, Lu HX, Yang H & Liu WC, Overexpression of FOXM1 predicts poor prognosis and promotes cancer cell proliferation, migration and invasion in epithelial ovarian cancer. *J Transl Med*, 12 (2014) 1.

33 Lee Y, Kim KH, Kim DG, Cho HJ, Kim Y, Rheey J, Shin K, Seo YJ, Choi YS & Lee JI, FoxM1 promotes stemness and radio-resistance of glioblastoma by regulating the master stem cell regulator Sox2. *PloS one*, 10 (2015) e0137703.

34 Buchner M, Park E, Klemm L, Geng H, Kopanja D, Raychaudhuri P & Muschen M, FOXM1 Mediates Drug-Resistance and Represents a Therapeutic Target in Pre-B Acute Lymphoblastic Leukemia. *Blood*, 124 (2014) 790.

35 Li L, Wu D, Yu Q, Li L & Wu P, Prognostic value of FOXM1 in solid tumors: a systematic review and meta-analysis. *Oncotarget*, 8 (2017) 32298.

36 Koo CY, Muir KW & Lam EWF, FOXM1: From cancer initiation to progression and treatment. *BBA-Gene Regul Mech*, 1819 (2012) 28.

37 Kalathil D, John S & Nair AS, FOXM1 and cancer: faulty cellular signaling derails homeostasis. *Front Oncol*, 10 (2021) 626836.

38 Yang K, Jiang L, Hu Y, Yu J, Chen H, Yao Y & Zhu X, Short hairpin RNA-mediated gene knockdown of FOXM1 inhibits the proliferation and metastasis of human colon cancer cells through reversal of epithelial-to-mesenchymal transformation. *J Exp Clin Cancer Res*, 34 (2015) 1.

39 Dey P, Wang A, Ziegler Y, Kim SH, El-Ashry D, Katzenellenbogen JA & Katzenellenbogen BS, Suppression of tumor growth, metastasis & signaling pathways by reducing FOXM1 activity in triple negative breast cancer. *Cancers*, 12 (2020) 2677.

40 Kwok JMM, Peck B, Monteiro LJ, Schwenen HD, Millour J, Coombes RC, Myatt SS & Lam EWF, FOXM1 confers acquired cisplatin resistance in breast cancer cells. *Mol Cancer Res*, 8 (2010) 24.

41 Carr JR, Park HJ, Wang Z, Kiefer MM & Raychaudhuri P, FoxM1 mediates resistance to herceptin and paclitaxel. *Cancer Res*, 70 (2010) 5054.

42 Hegde NS, Sanders DA, Rodriguez R & Balasubramanian S, The transcription factor FOXM1 is a cellular target of the natural product thiostrepton. *Nat chem*, 3 (2011) 725.

43 Gormally MV, Dexheimer TS, Marsico G, Sanders DA, Lowe C, Matak-Vinković D, Michael S, Jadhav A, Rai G & Maloney DJ, Suppression of the FOXM1 transcriptional programme *via* novel small molecule inhibition. *Nat commun*, 5 (2014) 5165.

44 Shukla S, Milewski D, Pradhan A, Rama N, Rice K, Le T, Flick MJ, Vaz S, Zhao X & Setchell KD, The FOXM1 inhibitor RCM-1 decreases carcinogenesis and nuclear β-catenin. *Mol Cancer Ther*, 18 (2019) 1217.

45 Raghuwanshi S, Zhang X, Arbieva Z, Khan I, Mohammed H, Wang Z, Domling A, Camacho CJ & Gartel AL, Novel FOXM1 inhibitor STL001 sensitizes human cancers to a broad-spectrum of cancer therapies. *Cell Death Dis*, 10 (2024) 211.

46 Wang K, Dai X, Yu A, Feng C, Liu K & Huang L, Peptide-based PROTAC degrader of FOXM1 suppresses cancer and decreases GLUT1 and PD-L1 expression. *J Exp Clin Cancer Res*, 41 (2022) 289.

47 Chesnokov MS, Halasi M, Borhani S, Arbieva Z, Shah BN, Oerlemans R, Khan I, Camacho CJ & Gartel AL, Novel FOXM1 inhibitor identified via gene network analysis induces autophagic FOXM1 degradation to overcome chemoresistance of human cancer cells. *Cell Death Dis*, 12 (2021) 704.

48 Garner MM & Revzin A, The use of gel electrophoresis to detect and study nucleic acid—protein interactions. *Trends Biochem Sci*, 11 (1986) 395.

49 Das PM, Ramachandran K, vanWert J & Singal R, Chromatin immunoprecipitation assay. *BioTechniques*, 37 (2004) 961.

50 Royer CA, Fluorescence spectroscopy. *Protein stability and folding: Theory and practice*, 40 (1995) 65.

51 Littler D, Alvarez-Fernandez M, Stein A, Hibbert R, Heidebrecht T, Aloy P, Medema R & Perrakis A, Structure of the FoxM1 DNA-recognition domain bound to a promoter sequence. *Nucleic Acids Res*, 38 (2010) 4527.

52 Bugnon M, Röhrig UF, Goullieux M, Perez MA, Daina A, Michielin O & Zoete V, SwissDock 2024: major enhancements for small-molecule docking with Attracting Cavities and AutoDock Vina. *Nucleic Acids Res*, 52 (2024) gkae300.